Group 11 Metal Complexes of N-Heterocyclic Carbene Ligands: Nature of the Metal−Carbene Bond

Xile Hu, Ingrid Castro-Rodriguez, Kristian Olsen, and Karsten Meyer*

Department of Chemistry and Biochemistry, Mail Code 0358, University of California, San Diego, 9500 Gilman Drive, La Jolla, California 92093-0358

Received September 22, 2003

The silver complex of the tripodal N-heterocyclic carbene ligand $TIME^{Me}$, $[(TIME^{Me})_2Ag_3](PF_6)_3$ (**3**), reacts with copper(I) bromide and (dimethyl sulfide)gold(I) chloride to yield the corresponding D_3-symmetrical copper(I) and gold(I) complexes $[(TIME^{Me})_2Cu_3](PF_6)_3$ (**4**) and $[(TIME^{Me})_2Au_3](PF_6)_3$ (**5**). Single-crystal X-ray diffraction, spectroscopic, and computational studies of this series of metal NHC complexes are described. The group 11 metal complexes of the $TIME^{Me}$ ligand exhibit isostructural geometries, with three metal ions bridging two of the $TIME^{Me}$ ligands. Each metal ion is linearly coordinated to two carbene centers, with each of the carbenoid carbons stemming from a different ligand. Overall, the molecules possess D_3 symmetry. The electronic structure of these newly synthesized compounds was elucidated with the aid of DFT calculations. In contrast to the common assumption that NHCs are pure σ-donor ligands, our calculations reveal the existence of both σ- and π-type interactions between the metal ions and the carbenoid carbons. A study of the closely related D_{2d}-symmetrical species $Pd(CN_2Bu^t_2C_2H_2)_2$ (**6**) and the simplified D_{2h}-symmetrical model complexes $M(IM^{Me}C:)_2$ (**8**−**10**; M = Ag, Cu, Au) allowed for quantitative comparison of the two different types of bonding interactions. It was found that π-back-bonding interactions in these diaminocarbene model species contribute to approximately 15−30% of the complexes' overall orbital interaction energies.

Introduction

Since the discovery of their remarkable activity in homogeneous catalysis,[1−4] enormous research interest has emerged in the chemistry of metal complexes supported by N-heterocyclic carbenes (NHCs).[5] Numerous metal NHC complexes have been synthesized, and their structures have been determined by single-crystal X-ray diffraction studies.[1,2,6] In many cases, single M−C bonds were observed, which in most reports has led to the assumption that NHCs are pure σ-donor ligands. The successful synthesis of main-group-metal NHC complexes, such as the beryllium tris(carbene) complex $[(IMC:)_3Be(Cl)]Cl$,[7] is regarded as empirical evidence for this bonding model.[8] However, it is noteworthy that NHC complexes of main-group metals, such as lithium,[9] beryllium,[7] and thallium(I),[10] are often air, moisture, and even temperature sensitive, while NHC complexes of transition metals (TMs) generally exhibit much higher stabilities. The above-mentioned main-group-metal NHC complexes obviously are not capable of back-donating electrons into the carbene p−π orbitals, which might be a reason for their relatively weak M−C bonds. While NHCs have been almost exclusively referred to as pure σ-donors in recent years, Taube and Clarke reported as early as 1975 the existence of π-back-bonding in ruthenium(II) NHC (carbon-bound xanthine) complexes.[11] Several recent theoretical studies also suggest various degrees of π-bonding in transition-metal NHC complexes.[12−15] For example, density functional theory (DFT) calculations revealed that metal-to-ligand π-back-bonding effects allowed for the isolation of an air-stable vanadium(V) trichloro oxo NHC complex.[14] In addition, a DFT study suggested the involvement of metal−carbene d−pπ hybrid orbitals in transition states of an alkylcarbene elimination from Pd(II) NHC complexes.[16] However, rigorous computational studies on crystallographically characterized metal NHC complexes are still

* To whom correspondence should be addressed. E-mail: kmeyer@ucsd.edu.

(1) Bourissou, D.; Guerret, O.; Gabbai, F. P.; Bertrand, G. *Chem. Rev.* **2000**, *100*, 39−91.
(2) Herrmann, W. A. *Angew. Chem., Int. Ed.* **2002**, *41*, 1291−1309.
(3) Huang, J. K.; Stevens, E. D.; Nolan, S. P.; Petersen, J. L. *J. Am. Chem. Soc.* **1999**, *121*, 2674−2678.
(4) Scholl, M.; Ding, S.; Lee, C. W.; Grubbs, R. H. *Org. Lett.* **1999**, *1*, 953−956.
(5) Arduengo, A. J.; Harlow, R. L.; Kline, M. *J. Am. Chem. Soc.* **1991**, *113*, 361−363.
(6) Herrmann, W. A.; Kocher, C. *Angew. Chem., Int. Ed. Engl.* **1997**, *36*, 2163−2187.
(7) Herrmann, W. A.; Runte, O.; Artus, G. *J. Organomet. Chem.* **1995**, *501*, C1−C4.
(8) Frohlich, N.; Pidun, U.; Stahl, M.; Frenking, G. *Organometallics* **1997**, *16*, 442−448.
(9) Frankell, R.; Birg, C.; Kernbach, U.; Habereder, T.; Noth, H.; Fehlhammer, W. P. *Angew. Chem., Int. Ed.* **2001**, *40*, 1907−1910.
(10) Nakai, H.; Tang, Y. J.; Gantzel, P.; Meyer, K. *Chem. Commun.* **2003**, 24−25.
(11) Clarke, M. J.; Taube, H. *J. Am. Chem. Soc.* **1975**, *97*, 1397−1403.
(12) Boehme, C.; Frenking, G. *Organometallics* **1998**, *17*, 5801−5809.
(13) Deubel, D. V. *Organometallics* **2002**, *21*, 4303−4305.
(14) Abernethy, C. D.; Codd, G. M.; Spicer, M. D.; Taylor, M. K. *J. Am. Chem. Soc.* **2003**, *125*, 1128−1129.
(15) Termaten, A. T.; Schakel, M.; Ehlers, A. W.; Lutz, M.; Spek, A. L.; Lammertsma, K. *Chem. Eur. J.* **2003**, *9*, 3577−3582.
(16) McGuinness, D. S.; Saendig, N.; Yates, B. F.; Cavell, K. J. *J. Am. Chem. Soc.* **2001**, *123*, 4029−4040.

10.1021/om0341855 CCC: $27.50
Publication on Web 01/14/2004

Scheme 1. Synthesis of Group 11 Metal Complexes of the TIME^{Me} Ligand

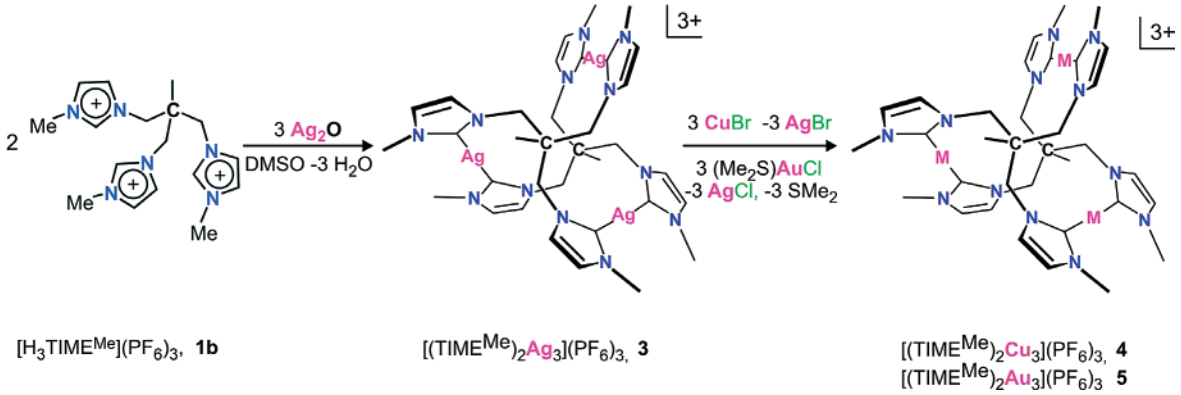

scarce and, as a result, the detailed nature of metal−carbene bonds remains to be unveiled.

During the past decade, quantum-mechanical methods have gained widespread acceptance in the study of TM compounds.[17−19] This is mostly due to the recent development of modern density functional theories. Analyzing the calculated electronic structures resulting from DFT calculations provides insight into the nature of bonding in TM compounds.[19,20] Bonding models based on quantum-mechanical concepts have thus been developed to qualitatively understand and, furthermore, predict the structures and reactivities of inorganic and organometallic compounds, such as metal carbonyl complexes,[21] Fischer-type and Schrock-type metal carbene complexes,[21−24] and alkene and alkyne π-complexes,[25,26] as well as an unusual silver phosphorus compound, $[Ag(\eta^2\text{-}P_4)_2]^+$.[27] Surprisingly, only very few quantum-mechanical investigations on metal NHC complexes, especially TM NHC complexes, have been reported.[12−15,28] This is in contrast to their vast popularity in the field of organometallic chemistry.

In the course of developing tris(carbene) ligand systems for transition-metal coordination and subsequent application in small molecule activation chemistry,[29−31] we recently synthesized the novel tripodal polycarbene ligand system 1,1,1-tris[(3-methylimidazol-2-ylidene)-methyl]ethane (TIME^{Me}) and its corresponding silver complex.[29] The silver carbene complex has proven to be a useful carbene transfer reagent for the otherwise unstable free polycarbene TIME^{Me}. We here report the synthesis of Cu(I) and Au(I) complexes of the polycarbene ligand TIME^{Me} via Ag(I) carbene transfer routes.[32] Our previously reported DFT study on the D_3-symmetrical $[(TIME^{Me})_2Ag_3]^{3+}$ complex suggested the existence of π-interaction in the silver carbene moieties.[29] The successful synthesis of the analogous copper and gold TIME^{Me} complexes prompted our interest in a comprehensive DFT investigation of these group 11 complexes and analogous, closely related species. The main goal of the DFT study reported herein is to provide further insight into the nature of bonding in NHC complexes and aims at defining the concept of π-interactions in metal−NHC bonding in a more general manner.

Results and Discussion

Ligand Synthesis and Characterization. The imidazolium precursor 1,1,1-[tris(3-methylimidazolium-1-yl)methyl]ethane tribromide (**1a**; $[H_3TIME^{Me}](Br_3)$) was synthesized by quaternization of *N*-methylimidazole with 1,1,1-tris(bromomethyl)ethane. Treatment of **1a** with ammonium hexafluorophosphate in methanol afforded the precipitation of pure $[H_3TIME^{Me}](PF_6)_3$ (**1b**). The most prominent features of the ^1H and ^{13}C spectra of **1a**,**b** are the resonances for the imidazolium protons at around 9 ppm and the corresponding imidazolium carbons at around 138 ppm.

Treatment of **1a**,**b** with strong bases such as *n*-butyllithium, potassium *tert*-butoxide, and benzylpotassium yields the free carbene **2**, 1,1,1-[tris(3-methylimidazol-2-ylidene)methyl]ethane ([TIME^{Me}]), in situ. Attempts to isolate **2**, however, led to reddish, polymeric species that exhibit complicated NMR spectra. Instead, formation of **2** was confirmed by trapping the free carbene with copper triflate and isolating the resulting copper complex (vide infra).

Complex Synthesis and Characterization. We reported previously that treatment of $[TIME^{Me}](PF_6)_3$ (**1b**) with Ag_2O in DMSO at 75 °C provides ready access to the stable silver complex $[(TIME^{Me})_2Ag_3](PF_6)_3$ (**3**), an effective carbene transfer reagent (Scheme 1). Reaction of **3** with copper(I) bromide and (dimethyl sulfide)-gold(I) chloride under a dry N_2 atmosphere yields the isostructural and isomorphous corresponding copper(I) and gold(I) complexes $[(TIME^{Me})_2Cu_3](PF_6)_3$ (**4**) and $[(TIME^{Me})_2Au_3](PF_6)_3$ (**5**). Following these reactions by

(17) Davidson, E. R. *Chem. Rev.* **2000**, *100*, 351−352.
(18) Torrent, M.; Sola, M.; Frenking, G. *Chem. Rev.* **2000**, *100*, 439−493.
(19) Frenking, G.; Frohlich, N. *Chem. Rev.* **2000**, *100*, 717−774.
(20) Frenking, G.; Wichmann, K.; Frohlich, N.; Loschen, C.; Lein, M.; Frunzke, J.; Rayon, V. M. *Coord. Chem. Rev.* **2003**, *238*, 55−82.
(21) Jacobsen, H.; Ziegler, T. *Inorg. Chem.* **1996**, *35*, 775−783.
(22) Vyboishchikov, S. F.; Frenking, G. *Chem. Eur. J.* **1998**, *4*, 1428−1438.
(23) Vyboishchikov, S. E.; Frenking, G. *Chem. Eur. J.* **1998**, *4*, 1439−1448.
(24) Jacobsen, H.; Ziegler, T. *Organometallics* **1995**, *14*, 224−230.
(25) Li, J. A.; Schreckenbach, G.; Ziegler, T. *Inorg. Chem.* **1995**, *34*, 3245.
(26) Kovacs, A.; Frenking, G. *Organometallics* **1999**, *18*, 887−894.
(27) Deubel, D. V. *J. Am. Chem. Soc.* **2002**, *124*, 12312−12318.
(28) Green, J. C.; Scurr, R. G.; Arnold, P. L.; Cloke, F. G. N. *J. Chem. Soc., Chem. Commun.* **1997**, 1963−1964.
(29) Hu, X.; Tang, Y.; Gantzel, P.; Meyer, K. *Organometallics* **2003**, *22*, 612−614.
(30) Hu, X.; Castro-Rodriguez, I.; Meyer, K. *Organometallics* **2003**, *22*, 3016−3018.
(31) Hu, X.; Castro-Rodriguez, I.; Meyer, K. *J. Am. Chem. Soc.* **2003**, *125*, 12237−12245.
(32) Wang, H. M. J.; Lin, I. J. B. *Organometallics* **1998**, *17*, 972−975.

Table 1. NMR Data of the M−TIME^{Me} Carbene Complexes and the Corresponding Imidazolium Salt (in ppm), Recorded in DMSO at 25 °C

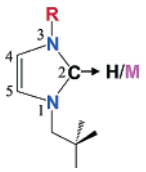

	1b	3	4	5
H(2)	9.12			
H(4)/H(5)	7.8/7.7	7.6/7.5	7.5/7.4	7.6/7.5
C(2)	137.8	182.5	180.0	183.8
C(4)/C(5)	123.5	123.6/123.2	123.0	123.6

NMR spectroscopy indicated that the carbene ligand transfer reaction proceeds quantitatively.

However, when the reactions are conducted in air, only the imidazolium salts are formed, suggesting that the reaction proceeds via a free carbene intermediate. Similar observations of a free carbene intermediate were previously reported for the formation of a tungsten diaminocarbene complex via a transmetalation reaction.[32]

Alternatively, in situ trapping of free carbene **2** with copper(I) triflate in THF afforded the corresponding $[(TIME^{Me})_2Cu_3]^{3+}$ complex as the triflate salt, which can be further converted into **4** by means of anion exchange.

Slow ether diffusion into acetonitrile solutions of complexes **4** and **5** afforded colorless crystals that were characterized by NMR, IR, UV/vis spectroscopy, and X-ray diffraction analysis.

In general, the ^{1}H spectra of **3**−**5** are very similar (Table 1). The resonances for the 4H/5H protons of the imidazole ring backbone were observed at 7.6/7.5 ppm for **3**, 7.5/7.4 ppm for **4**, and 7.6/7.5 ppm for **5**. In comparison to the analogous nuclei of the imidazolium salts (7.9/7.8 ppm for **1a**, 7.8/7.7 ppm for **1b**), all ring-backbone resonances are shifted slightly upfield. In the ^{13}C spectra, the chemical shifts for the carbenoid carbons were found at 182.5 (**3**), 180.0 (**4**), and 183.8 (**5**) ppm, respectively. These results are similar to those of other reported group 11 metal NHC complexes.[33−36] Silver−carbon coupling, however, was not observed, indicating the fluxional behavior of **3** in solution.[32,35]

In the infrared vibrational spectra, the characteristic N−C−N stretching frequencies,[37] ν(N−C−N), are 1570 cm^{-1} for **3**, 1571 cm^{-1} for **4**, and 1572 cm^{-1} for **5**. The vibrational bands at around 3200−3100 cm^{-1} can be assigned to the ν(C−H) stretching vibrations of the heterocycle, and bands between 3000 and 2900 cm^{-1} are known to correspond to the ν(C−H) stretching vibration of the aliphatic groups. The electronic absorption spectra of **3**−**5** recorded in acetonitrile are characterized by intense absorption bands (λ/nm, ϵ/M^{-1} cm^{-1}) in the ultraviolet region at 210 (81 000), 224 (77 000), 240 (58 000), and 364 (2000) for **3**, 210 (46 000), 256 (24 000), and 270 nm (22 000) for **4**, and 210 (84 000), 216 (76 000), 234 (74 000), 246 (82 000), 260 (73 000), and 290 nm (23 000) for **5** (Figure S1, Supporting Information). The spectrum of the corresponding ligand salt exhibits only one absorption band at 214 nm (13 000). Although the assignment of these absorption bands remains largely equivocal, we suggest that they originate from ligand-centered as well as ligand-to-metal and metal-to-ligand charge-transfer transitions.

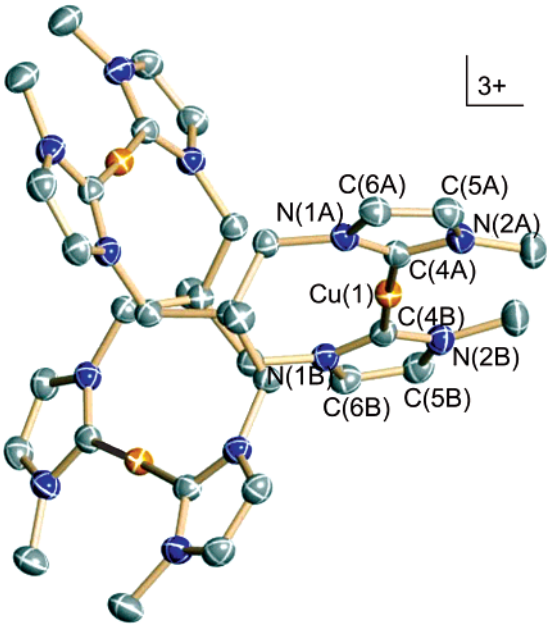

Figure 1. Solid-state molecular structure of $[Cu_3(TIME^{Me})_2](PF_6)_3$ in crystals of **4**. Counteranions and hydrogen atoms are omitted for clarity; thermal ellipsoids are given at 50% probability. Selected bond distances (Å) and angles (deg): Cu(1)−C(4A) = 1.9124(16), C(4A)−N(1A) = 1.363(2), C(4A)−N(2A) = 1.350(2), C(5A)−C(6A) = 1.349(2); C(4A)−Cu(1)−C(4B) = 177.70(9), N(1A)−C(4A)−N(2A) = 103.78(13).

Table 2. Selected Bond Lengths (Å) and Angles (deg) for Group 11 Metal Complexes of the TIME^{Me} Ligand, $[(TIME^{Me})_2M_3](PF_6)_3$ (M = Ag (3), Cu (4), Au (5))

	3	4	5
M−C(4A)	2.082(2)	1.9124(16)	2.035(12)
C(4A)−N(1A)	1.359(3)	1.363(2)	1.352(13)
C(4A)−N(2A)	1.347(3)	1.350(2)	1.332(13)
C(5A)−C(6A)	1.341(4)	1.349(2)	1.343(17)
M−M	5.54	5.51	5.54
C(4A)−M−C(4B)	178.56(13)	177.70(9)	177.7(6)
N(1A)−C(4A)−N(2A)	104.3(2)	103.78(13)	105.3(8)

Single-crystal X-ray diffraction studies confirmed the isostructural geometries for complexes **3**−**5** (Figure 1, Figure S2 (Supporting Information), and Table 2).[38] In each of the three solid-state structures, an M_3L_2 composition was found, with three metal ions bridging two TIME^{Me} ligands through each of the three pendant arms. Each metal ion is coordinated to two of the carbenoid carbon atoms, with each carbene center stemming from a different ligand. All structures exhibit D_3 symmetry, with a 3-fold axis passing through the anchoring C atoms of the two ligands.

(33) Arnold, P. L.; Scarisbrick, A. C.; Blake, A. J.; Wilson, C. *Chem. Commun.* **2001**, 2340−2341.
(34) Arduengo, A. J.; Dias, H. V. R.; Calabrese, J. C.; Davidson, F. *Organometallics* **1993**, *12*, 3405−3409.
(35) Garrison, J. C.; Simons, R. S.; Talley, J. M.; Wesdemiotis, C.; Tessier, C. A.; Youngs, W. J. *Organometallics* **2001**, *20*, 1276−1278.
(36) Guerret, O.; Sole, S.; Gornitzka, H.; Teichert, M.; Trinquier, G.; Bertrand, G. *J. Am. Chem. Soc.* **1997**, *119*, 6668−6669.
(37) Frankel, R.; Kniczek, J.; Ponikwar, W.; Noth, H.; Polborn, K.; Fehlhammer, W. P. *Inorg. Chim. Acta* **2001**, *312*, 23−39.

(38) The crystal structure of complex **3** was communicated previously in ref 43. The metric parameters are listed here to compare with those of the isostructural complexes **4** and **5**.

Compound **4** represents a rare example of a crystallographically characterized homoleptic copper(I) NHC complex. In the solid-state structure (Figure 1), the average Cu−C distance is 1.9124(16) Å, which is within the range of reported values for typical copper(I) NHC complexes (1.880−1.963 Å).[33,39] Similarly, in the crystal structure of **5** (Figure S2, Supporting Information), the average Au−C bond distance of 2.035(15) Å is consistent with the values reported for other related two-coordinate gold carbene complexes.[40−42] The carbene copper entities are nearly linear, with a C−Cu−C′ bond angle of 177.70(9)°, comparable to those of its analogues: 178.56(13)° in **3** and 177.7(6)° in **5**. Intermolecular metal−metal interactions cannot be observed for this series of trinuclear complexes, with the shortest metal−metal distances being 5.54, 5.51, and 5.54 Å for **3**−**5**, respectively.

The imidazole units in the structures of **3**−**5** exhibit typical features of coordinated NHC ligands (Table 2). Specifically, the average $C_{carbene}$−N bond distances, $d(N-C_{carbene})_{av}$, increased from 1.326 Å in the imidazolium salt **1a** to 1.353 Å in complex **3**, 1.357 Å in **4**, and 1.346 Å in **5**. The N−$C_{carbene}$−N ring angles are significantly decreased from 108.5° in **1a**[29] to 104.3° in **3**, 103.8° in **4**, and 105.3° in **5**. Such changes are well documented in the literature[2] and have been attributed to decreased π-delocalization in the five-membered ring[6] and increased p character of the carbenoid carbon,[43] resulting from deprotonation and subsequent coordination. Additionally, small decreases of the $C_{carbene}$−N bond distances and increases of N−$C_{carbene}$−N bond angles, going from Cu(I), Ag(I) to Au(I) NHC complexes, were observed. This is in agreement with the trends that previously have been found for NHC complexes of the 3d, 4d, and 5d transition-metal series.[6] The two imidazole rings coordinated to the same metal ion are nearly coplanar with dihedral angles of 6.4° (Ag), 7.7° (Cu), and 6.7° (Au).

The fact that the tripodal carbene system $TIME^{Me}$ forms η^2-μ^3 complexes instead of simple tridentate η^3 metal complexes with group 11 metal ions is probably due to the flexibility of the ligand. Three condensed eight-membered rings of a hypothetical 1:1 complex would exhibit significantly lower stability than the more common five-, six-, or seven-membered rings of tris(pyrazolyl) or tris(phosphine) ligands and, thus, likely is entropically disfavored. Similarly, the tris(pyrazolyl) analogue of the $TIME^{Me}$ ligand, 1,1,1-[tris(pyrazol-1-yl)methyl]ethane, reportedly acts as a bidentate chelator.[44]

DFT Studies. All calculations were carried out using the ADF program suite at the BP86 level with relativistic effects accounted for by ZORA.[45−47] Geometry optimizations and single-point calculations were carried out for complexes **3**−**5** and the closely related palladium complex $Pd(CN_2Bu^t_2C_2H_2)2$ (**6**).[48] Calculations carried out on the free carbene 1,3-dimethylimidazol-2-ylidene (**7**, **Im**)[49] served as a starting point for the construction of molecular orbital diagrams (vide infra). The metal−ligand bonding interactions were analyzed by using the energy-decomposition scheme introduced by Ziegler and Rauk.[50,51] The energy-decomposition analyses were carried out on the D_3-symmetrical complexes **3**−**5**, the D_{2d}-symmetrical complex **6**, and simplified model complexes for **3**−**5**, namely the D_{2h}-symmetrical complexes $M(IM^{Me}C:)_2$, (M = Ag (**8**), Cu (**9**), Au (**10**); $IM^{Me}C:$ = 1,3-dimethylimidazol-2-ylidene) (Chart 1).

Chart 1

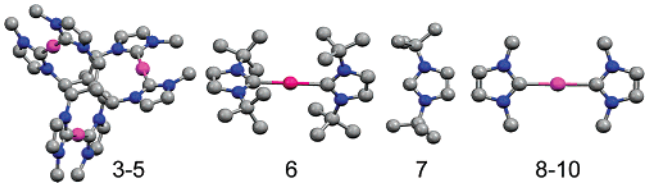

1. Optimized Geometries. The calculations result in structural parameters that reproduce the experimentally determined bond lengths and angles of complexes **3**−**6** (Table 3). Even the small decrease in the $C_{carbene}$−N bond distances and increase in N−$C_{carbene}$−N bond angles on going from Cu to Ag and Au are observed.

The structure of the free carbene 1,3-dimethylimidazol-2-ylidene (**Im**, **7**) is unknown; however, the calculated structure is in good agreement with those of the crystallographically characterized mesityl and adamantyl derivatives.[5,49] For example, the calculations resulted in an average N−$C_{carbene}$ bond length of 1.373 Å, which is comparable to 1.370 Å in 1,3-di-1-adamantylimidazol-2-ylidene[5] and 1.368 Å in 1,3-bis(2,4,6-trimethylphenyl)-imidazol-2-ylidene.[49] Also, the calculated N−$C_{carbene}$−N bond angle of 101.6° agrees well with the X-ray crystallographically determined 102.2 and 101.4°.

2. Bonding in the Metal NHC Complexes. I. Molecular Orbital Analysis. All metal−ligand interactions in complexes **3**−**6** were analyzed using a "fragment approach". This approach applied to complex **4** with three copper ions and two $TIME^{ME}$ ligands arranged in D_3 symmetry, for instance, results in a molecular orbital interaction diagram built from an M_3 fragment and an L_2 fragment of the M_3L_2 complex. Analysis of the corresponding molecular orbitals (MOs) allows for deriving σ-bonding and π-back-bonding models, describing the metal−ligand electronic interactions involved. The complicated MOs of the L_2 fragment are easier to understand when correlated with those of the much simpler free carbene **7**, followed by superimposing D_3 symmetry.

The orbital energy diagram of **7** is shown in Figure 2 (left). The highest occupied molecular orbital 19A

(39) Tulloch, A. A. D.; Danopoulos, A. A.; Kleinhenz, S.; Light, M. E.; Hursthouse, M. B.; Eastham, G. *Organometallics* **2001**, *20*, 2027−2031.
(40) Lee, K. M.; Lee, C. K.; Lin, I. J. B. *Angew. Chem., Int. Ed. Engl.* **1997**, *36*, 1850−1852.
(41) Raubenheimer, H. G.; Olivier, P. J.; Lindeque, L.; Desmet, M.; Hrusak, J.; Kruger, G. J. *J. Organomet. Chem.* **1997**, *544*, 91−100.
(42) Wang, H. M. J.; Chen, C. Y. L.; Lin, I. J. B. *Organometallics* **1999**, *18*, 1216−1223.
(43) Arduengo, A. J. *Acc. Chem. Res.* **1999**, *32*, 913−921.
(44) Jacobi, A.; Huttner, G.; Winterhalter, U.; Cunskis, S. *Eur. J. Inorg. Chem.* **1998**, 675−692.
(45) ADF2002.01; SCM, Theoretical Chemistry, Vrijie Universiteit: Amsterdam, The Netherlands.
(46) te Velde, G.; Bickelhaupt, F. M.; Baerends, E. J.; Guerra, C. F.; Van Gisbergen, S. J. A.; Snijders, J. G.; Ziegler, T. *J. Comput. Chem.* **2001**, *22*, 931−967.
(47) Guerra, C. F.; Snijders, J. G.; te Velde, G.; Baerends, E. J. *Theor. Chim. Acta* **1998**, *99*, 391−403.
(48) Arnold, P. L.; Cloke, F. G. N.; Geldbach, T.; Hitchcock, P. B. *Organometallics* **1999**, *18*, 3228−3233.
(49) Arduengo, A. J.; Dias, H. V. R.; Harlow, R. L.; Kline, M. *J. Am. Chem. Soc.* **1992**, *114*, 5530−5534.
(50) Ziegler, T.; Rauk, A. *Theor. Chim. Acta* **1977**, *46*, 1−10.
(51) Ziegler, T.; Rauk, A. *Inorg. Chem.* **1979**, *18*, 1558−1565.

Table 3. Selected Structural Parameters for Geometry-Optimized Species 3−6 and 7[a]

	3		4		5		6		7
structural param	calcd	exptl	calcd	exptl	calcd	exptl	calcd	exptl	calcd
$M-C_{carb}$	2.087	2.082	1.901	1.912	2.054	2.028	2.057	2.041	
av $N-C_{carb}$	1.366	1.353	1.371	1.357	1.365	1.347	1.388	1.361	1.373
C═C	1.359	1.341	1.360	1.349	1.360	1.344	1.357	1.357	1.362
av N−C	1.390	1.384	1.387	1.380	1.389	1.395	1.389	1.374	1.394
$N-C_{carb}-N$	103.9	104.3	103.5	103.8	104.4	105.2	102.8	105.3	101.6
$C_{carb}-M-C'_{carb}$	177.6	178.6	176.9	177.7	177.5	177.6	180.0	180.0	

[a] Bond distances are given in Å and bond angles in deg. Crystallographically characterized parameters for complexes **3**−**6** are listed for comparison.

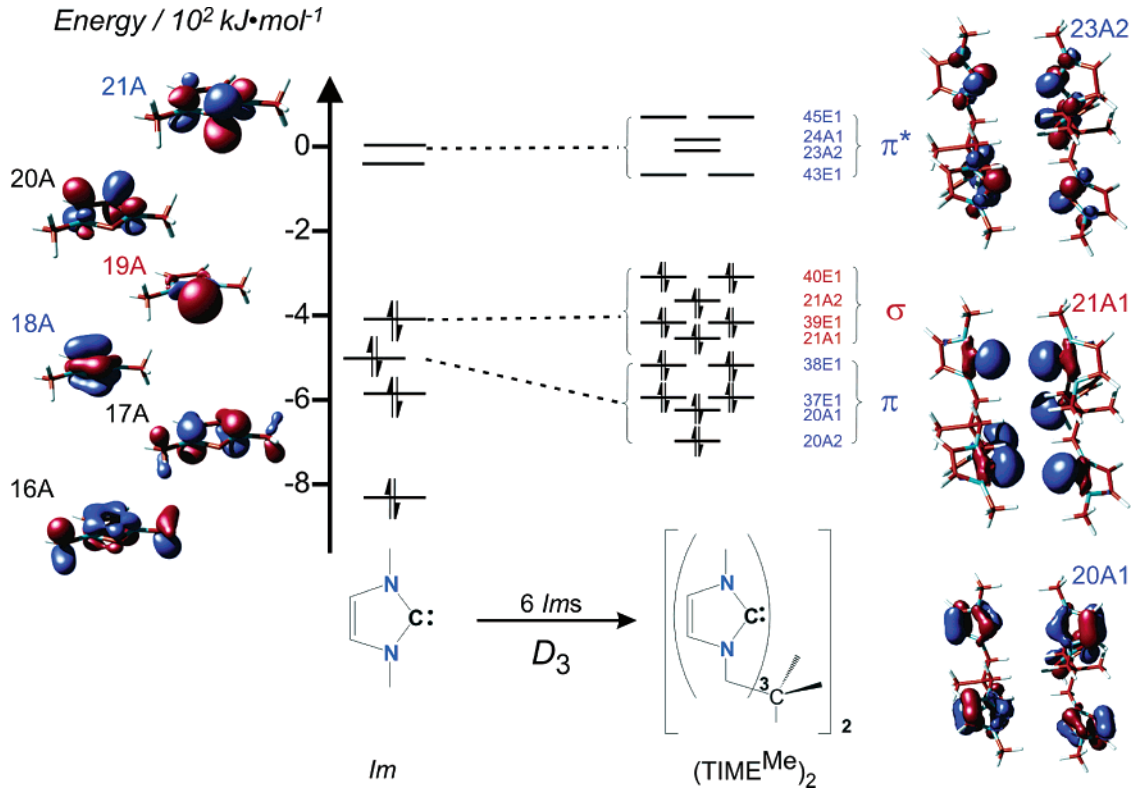

Figure 2. Orbital diagrams of carbene **Im** (left) and ligand fragment $(TIME^{Me})_2$ (right).

(HOMO) of **7** mainly contains the lone pair of the carbene center. This orbital has σ symmetry, and the energetic accessibility of this orbital allows NHC ligands to act as superb σ-donors. Near the HOMO, there are five more π-type orbitals that originate from the "aromaticity" of the imidazole ring.[6] Only two of these π-type orbitals, 18A and 21A, meet the requirements to interact with the MOs of the metal fragments of the complex. While occupied orbitals such as 18A alone do not result in net bonding with occupied metal d−π orbitals, they can mix with their unoccupied counterparts such as orbital 21A and interact with fully occupied metal d−π orbitals, resulting in overall stabilizing contributions (vide infra).

Considering all possible bonding interactions, a simplified orbital diagram of $(TIME^{Me})_2$ containing all relevant σ and π orbitals was constructed. The ligand fragment $(TIME^{Me})_2$ contains six imidazole rings arranged in D_3 symmetry. Therefore, the MOs of $(TIME^{Me})_2$ can be treated as linear combinations of six 19A-like σ-type orbitals and twelve 18A- and 21A-like π-type orbitals (Figure 2, right).

Accordingly, a qualitative molecular orbital correlation diagram of complex **4** is accessible by combining the two fragments $(TIME^{Me})_2$ and Cu_3 (Figure 3).[52] From this diagram it is apparent that both σ- and π-type bonding exist between the metal and the ligand fragments. Two types of σ bonding are involved (Figure 3). The dominant σ-contribution results from interaction of the ligand fragment σ orbitals with the $3d(z^2) + 4s$ hybrid orbitals of the metal fragment. A representative bonding orbital, 20A1, has 33% metal d + s character and 64% ligand character (Figure 4 left, bottom). The interaction between the ligand σ orbitals and the 4p(*z*) orbitals of the metal ions additionally produces a small but noticeable contribution. A representative bonding orbital with 14% metal p and 86% ligand character, 21A2, is shown in Figure 4 (left top). All ligand σ orbitals and the metal d orbitals are fully occupied; conversely, the metal s and p orbitals are empty. This results in an overall σ donation from the ligand to the metal fragment. Since the σ orbitals of the ligand fragment originate from the lone pairs of the carbene centers, the σ-bonding model described here is in accord with the well-known strong Lewis basicity of NHCs.

Importantly, the MO diagram shown in Figure 3 also reveals a detailed picture of the π-bonding interactions

(52) The unoccupied orbitals are omitted for clarity.

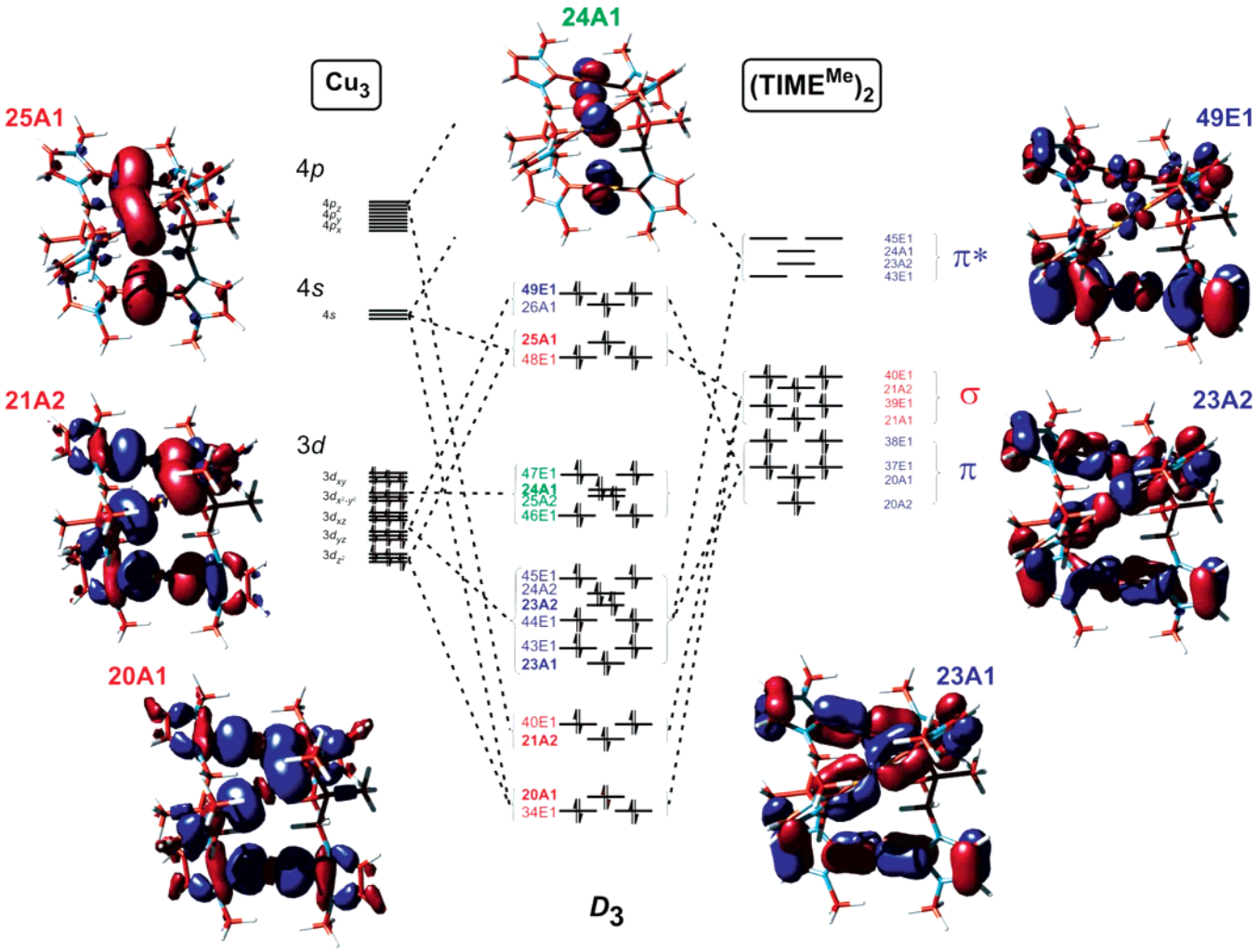

Figure 3. Qualitative orbital correlation diagram of complex **4**, $[(TIME^{Me})_2Cu_3]^{3+}$: σ-type orbitals are labeled in red, π-type orbitals are labeled in blue, and metal-based, nonbonding orbitals are labeled in green. The z axis is defined along the C−M−C entity.

in complex **4**. The metal d(xz)/d(yz) orbitals interact with both the π and π^* orbitals of the carbene ligands and form bonding, quasi-antibonding, and antibonding orbitals (Figure 3; orbitals with π symmetry are labeled in blue).[52] Typical π-type MOs are shown in Figure 4 (right). Orbital 23A1 has apparent bonding character, comprising 59% metal d and 41% ligand π/π^* contributions. Orbital 49E1 has quasi-antibonding character with 35% metal d and 65% ligand π/π^* contributions. This significant overlap of the fully occupied metal d(xz)/d(yz) orbitals and the partially empty ligand π/π^* orbitals,[53] stemming from the carbene p−π orbitals, is indicative of a π-back-bonding interaction between the metal ions and the NHCs.

This π bonding between the metal ions and NHC ligands is not limited to D_3-symmetrical complexes of group 11 metal ions such as **3**−**5**. In fact, calculations on complex **6** similarly revealed π interactions of various degrees. MO diagrams similar to that of complex **4** were constructed and analyzed for these complexes. The corresponding representative π-bonding MOs are presented in Figure 5.

II. Energy Decomposition Analysis. The nature of the M−$C_{carbene}$ bonds in complexes **3**−**6** was additionally explored using Ziegler and Rauk's energy-decomposition schemes[50,51] incorporated in the ADF program. The central element of such an analysis is the interaction energy (ΔE_{int}) between the bonding fragments. It is calculated as the energy difference between the geometry-optimized complex and the fragments with the frozen geometry of the complex. This energy difference can be broken down into three separate energy terms: $\Delta E_{int} = \Delta E_{Pauli} + \Delta E_{elst} + \Delta E_{orb}$. The Pauli energy term (ΔE_{Pauli}) refers to the four-electron destabilizing interactions between occupied orbitals, the electrostatic energy term (ΔE_{elst}) term gives the attractive electrostatic contributions, and the orbital energy term (ΔE_{orb}) gives the stabilizing orbital interaction energy arising when the Kohn−Sham orbitals relax to their optimal form. The latter energy term can be broken down into orbital contributions from different irreducible representations of the interacting system. This allows the calculation of stabilizing contributions stemming from orbitals with σ, π, or δ symmetry.

The bond energy of the complexes (ΔE_{bond}) was calculated by adding the preparation energy (ΔE_{prep}) to the

(53) The π orbitals of the ligand fragment are preoccupied, but the π^* orbitals are empty, and there is a mixing between these π and π^* orbitals when the ligands coordinate to the metal ions. Accordingly, the hybrid π/π^* orbitals are "partially empty" in the metal NHC complex.

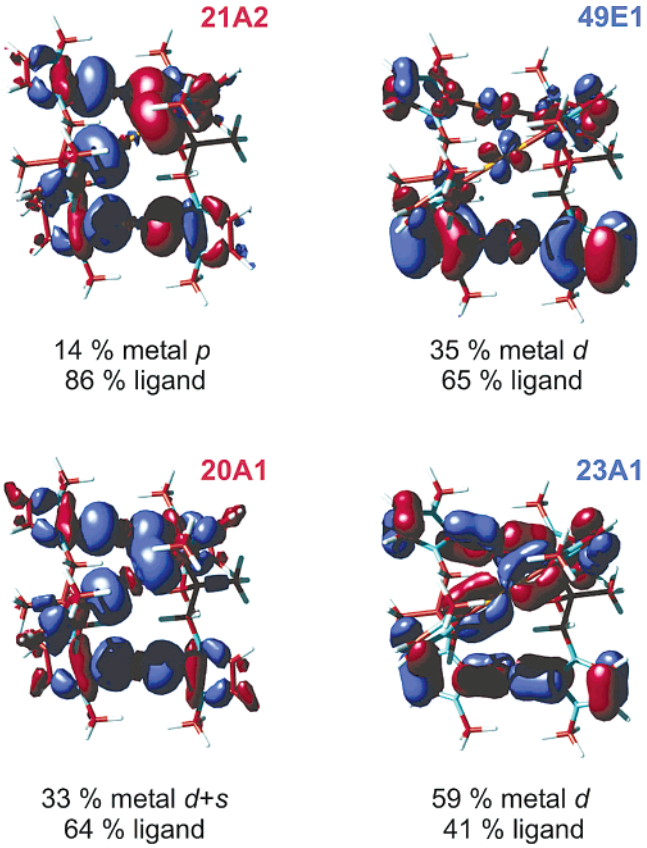

Figure 4. Representative molecular orbitals in complex **4**: (lef) σ-type orbitals; (right) π-type orbitals (see text for details).

interaction energy (ΔE_{int}) given by the above energy-decomposition analysis ($\Delta E_{bond} = \Delta E_{int} + \Delta E_{prep}$). The preparation energy is the energy that is necessary to promote two of the interacting fragments, e.g. A and B, from their equilibrium geometry to the geometry that they exhibit in the geometry-optimized species, e.g. AB. The bond dissociation energy (D_e) for each metal−carbene bond can in turn be deduced from the overall bond energy.

The results are summarized in Table 4. Our calculations reveal generally high M−$C_{carbene}$ bond dissociation energies, agreeing well with the stabilities of TM NHC complexes. The strongest M−C bond was found for complex **4**, in which each Cu−C bond has a D_e value of 81.45 kcal/mol. This value is even higher than that of the classical Fischer carbene complex $(CO)_5$W−CH(OH) (D_e = 75.0 kcal/mol at the CCSD(T) level).[22] In cationic complexes **3**−**5**, the metal−carbene bonds were found to be much stronger than in their isoelectronic neutral counterpart **6** (Table 3). The calculated D_e values in complexes **3**−**5** are slightly different from those found for the (ImC:)M(Cl) (M = Cu, Ag, Au) model system with D_e values of 67.4, 56.5, and 82.8 kcal/mol for the Cu(I), Ag(I), and Au(I) complexes, respectively.[12]

Partitioning the stabilizing orbital interaction energy (ΔE_{orb}) into contributions from different symmetries allows separation of σ and π interactions.[13,19,20,27,54] Generally, D_3-symmetrical group 11 metal NHC complexes with three metal ions in each molecule will not allow for such a separation. The mononuclear palladium bis(carbene) complex **6**, however, possesses D_{2d} symmetry with three main contributions to the orbital interaction energy stemming from different irreducible representations in the D_{2d} group (Figure 6). The major contribution arises from donation of carbene lone-pair electrons into the palladium 4d(z^2) + 5s hybrid (a1, −74.31 kcal/mol). The donation of carbene lone-pair electrons into the palladium 5p(z) orbital results in much less stabilization energy (b2, −5.94 kcal/mol). Overall, the sum of all σ-type contributions totals −79.35 kcal/mol. Notably, the interaction between the palladium d orbitals and the carbene p−π orbitals are also significant (e1, −36.28 kcal/mol) and cannot be neglected. The ratio of σ-donation/π-back-donation (d/b value) in **6** is 2.2, and the π bonding contributes 30% of the overall stabilizing orbital interaction energy (E_{orb} = −120.34 kcal/mol).

As mentioned earlier, quantitative separation of σ and π interaction energy in trinuclear complexes **3**−**5** is not possible, due to their D_3 symmetry. However, approximate results can be obtained by analysis of the simplified D_{2h}-symmetrical model compounds M($Im^{Me}C$:)$_2$, (M = Ag (**8**), Cu(**9**), Au(**10**)). The geometry of these mononuclear model compounds closely resembles the individual linear carbene−metal−carbene entities found for complexes **3**−**5** (see Chart 1). Calculations show that in these model complexes the main σ donations (a_{1g}) have energy contributions of −57.4 (**8**), −67.8 (**9**), and −73.7 kcal/mol (**10**), while the π interactions (b_{2g}) have energy contributions of −10.2 (**8**), −15.5 (**9**) and −12.6 kcal/mol (**10**). Thus, the d/b ratios are 5.6, 4.4, and 5.8, and therefore, the π bonding contributes to approximately 15%, 18%, and 15% of the overall stabilizing orbital interaction energy for Ag(I), Cu(I), and Au(I), respectively. The results are slightly different from that of hypothetical NHC ligand metal adducts (ImC:)M(Cl) (M = Ag, Cu, Au), with the d/b values being 6.6, 9.7, and 4.3 for Cu(I), Ag(I), and Au(I), respectively.[12] The smaller π-back-bonding contribution in complexes **8**−**10** relative to that in complex **6** might be attributed to the positive charge on the group 11 metal ions and the fact that in complexes **8**−**10** only one d−π orbital can be involved in the π-bonding, while in **6**, the two d−π orbitals can both take part in such interactions.

The above study leads to the conclusion that NHCs are not only excellent σ donors, but also fair π acceptors, even for the cationic closed-shell d^{10} metal centers discussed here. The magnitudes of such interactions, however, may vary. We generally do not agree with the use of a term such as "negligible" to describe the π-back-bonding in metal NHC complexes. It is true that, of the few calculated metal NHC complexes to date,[12,13,15] σ bonding accounts for more than 70% of the overall stabilizing orbital energy. Even so, it is important to recognize the potential π-acceptor properties of NHC ligands. As we and others[15] have shown with electron-rich metal centers, π-back-bonding can be significant and contributes up to 20−30% of the orbital interaction energy of a metal NHC complex: e.g. in the palladium complex **6** or in the iridium complex [Cp(NHC)-Ir=CH_2].[15] It is found that, in the NHC−Ir fragment of the latter complex, π back-bonding contributes to 20% of the covalent bonding energy of the fragment, while

(54) Massera, C.; Frenking, G. *Organometallics* **2003**, *22*, 2758−2765.

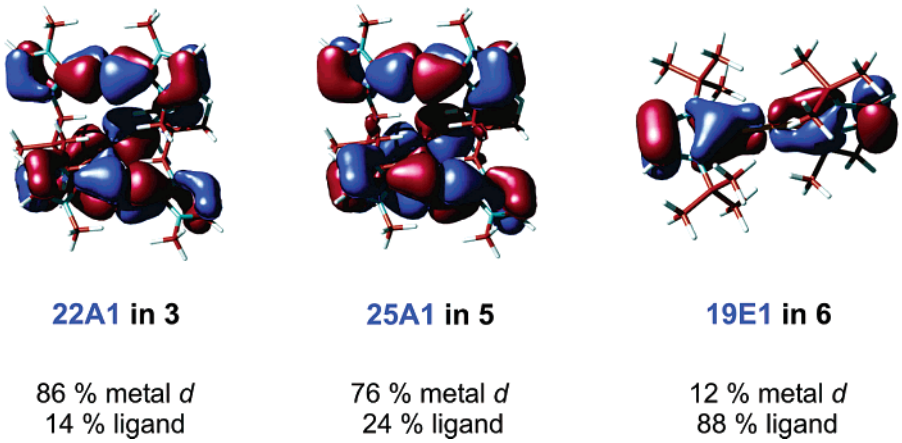

Figure 5. Representative π-type molecular orbitals in complexes **3**, **5**, and **6**.

Table 4. Energy Decomposition of the Metal NHC Complexes in the D_3 (3−5) and D_{2d} (6) Groups at the BP86 Level

		contribn (kcal/mol)			
param	descripn	**3**	**4**	**5**	**6**
ΔE_{Pauli}	Pauli repulsion	697.1	628.0	1066.3	323.6
ΔE_{elst}	electrostatic interaction	−827.7	−848.4	−1127.5	−289.2
ΔE_{orb}	stabilizing orbital interactions	−358.7	−428.8	−525.0	−120.3
ΔE_{int}	bond interaction energy	−467.8	−624.5	−558.2	−83.0
$\Delta E_{\text{prep\_m}}$	prep energy for the metal fragment	127.9	120.8	89.3	0
$\Delta E_{\text{prep\_l}}$	prep energy for the ligand fragment	8.9	14.9	11.7	8.08
ΔE_{bond}	bond energy	−330.9	−488.7	−457.2	−75.0
D_e(M−C)	BDE for each metal−carbene bond	55.2	81.5	76.2	37.5

in the Schrock-type carbene fragment {M=CH_2} (a benchmark fragment for the σ-bonding/π-back-bonding model), π back-bonding has a 25% contribution to its covalent bonding energy.[15]

Conclusion

In summary, we have synthesized a series of group 11 metal complexes of the tripodal N-heterocyclic carbene ligand system 1,1,1-[tris(3-methylimidazol-2-ylidene)methyl]ethane ([TIME^{Me}]). Single-crystal X-ray diffraction, spectroscopic, and computational studies of this series of metal complexes [(TIME^{Me})$_2$M$_3$](PF$_6$)$_3$ (M = Cu, Ag, Au) are described.

The group 11 metals form homoleptic trinuclear complexes with the polycarbene ligand TIME^{Me}. All complexes are isostructural and isomorphous and crystallize in the same rhombohedral $R\bar{3}c$ space group. The structures possess D_3 symmetry, with three metal ions bridging two of the TIME^{Me} ligands. Each metal ion is linearly coordinated to two carbene centers, with each carbenoid carbon stemming from a different ligand.

The electronic structure of these group 11 metal complexes was elucidated with the aid of molecular orbital analysis based on results from DFT calculations. The analysis reveals the expected σ-type interactions in addition to non-negligible π interactions between the electron-rich metal ions and the carbene p−π orbitals. Energy decomposition analysis of the closely related D_{2d}-symmetrical Pd complex Pd(CN$_2$Bu$^t_2$C$_2$H$_2$)$_2$ and the D_{2h}-symmetrical model complexes M(Im^{Me}C:)$_2$ (M = Ag, Cu, and Au) allowed for a quantitative comparison of π and σ contributions. It was found that the π-back-bonding interactions in these diaminocarbene species contribute to approximate 15−30% of the complexes' overall orbital interaction energies.

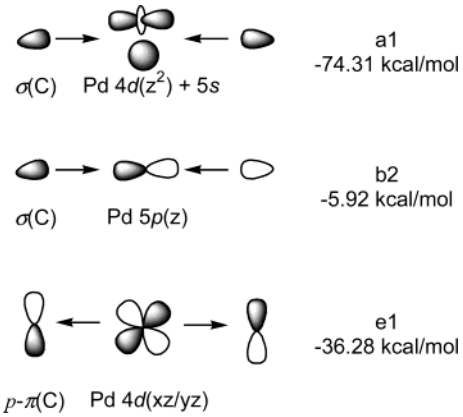

Figure 6. Main contributions of the irreducible representations to the stabilizing orbital-interaction energy (ΔE_{orb}) in Pd(CN$_2$Bu$^t_2$C$_2$H$_2$)$_2$ (**6**; D_{2d}).

This finding of non-negligible or even significant π-bonding interactions in metal NHC complexes is at first sight in astonishing contrast to the common assumption that NHC ligands are pure σ donors. However, the latter assumption has generally been based on the "single-bond" character of the M−C$_{\text{carbene}}$ interactions deduced from crystallographically determined bond distances. While it is customary, and often instructive, to correlate a given bond length with the bond order in a certain class of compounds, such correlation is purely empirical and by itself is not sufficient to corroborate the nature of any given metal−ligand interaction. Instead, for the investigation of π-back-bonding from the metal to the π* orbitals of NHC ligands it is more instructive to compare structural parameters of the imidazole rings in a series of isostructural NHC complexes containing electron-rich, less electron-rich, and electron-poor metal centers. If π back-bonding from metal to the NHC ligand exists, one would expect a decrease of the nitrogen-to-carbene π bonding and, thus, an increase of the C−N bond lengths for the more electron-rich metal centers. Extensive search in the Cambridge Crystallographic Data Centre (CCDC) actually does provide convincing structural evidence for

metal−NHC π back-bonding: for instance, comparison of structural parameters for the bis(carbene) complexes $(NHC^{Mes})_2M$ (with NHC^{Mes} = 1,3-dimesitylimidazol-2-ylidene, M = Ni(0), Ag(I), I^+).[34,55,56] These complexes are isostructural and bear the same set of NHC ligands; all structural data were collected at low temperature. It is apparent that from I^+ (electron poor, not capable of π back-bonding) to Ag^+ (less electron-rich, capable of π back-bonding) to Ni(0) (electron-rich, very capable of π-back-bonding), the average NHC C−N bond lengths increase from 1.346 Å in $[(NHC^{Mes})_2I]^+$ to 1.358 Å in $[(NHC^{Mes})_2Ag]^+$ to 1.375 Å in $[(NHC^{Mes})_2Ni]$. These structural changes provide indeed very definitive experimental evidence for the existence of metal−NHC π back-bonding. Nevertheless, quantum-mechanical calculations are straightforward and essential in unveiling the "true" nature of the metal−carbene bond. While some may argue that 15% of π bonding is "negligible", such simplification would certainly overlook the exact nature of the metal−NHC bond, as well as the potential role of metal−carbene π back-bonding in the diverse NHC chemistry.

Experimental Section

Methods and Procedures. Manipulation of air-sensitive compounds was performed under a controlled dry nitrogen atmosphere using standard Schlenk-line techniques and inert-gas gloveboxes (MBraun Labmaster by M. Braun, Inc.). Solvents were purified using a two-column solid-state purification system (Glasscontour System, Joerg Meyer, Irvine, CA), transferred to the glovebox without exposure to air, and stored over molecular sieves and/or sodium metal. NMR solvents were obtained from Cambridge Isotope Laboratories, degassed, and stored over activated molecular sieves prior to use. All NMR spectra were recorded at room temperature (20 °C) in d_6-benzene, d_3-acetonitrile, and d_6-DMSO solutions on Varian spectrometers operating at 400/300 MHz (^{1}H NMR) and 100 MHz (^{13}C NMR) and referenced to residual solvent peaks unless otherwise noted (δ in ppm). Infrared spectra (400−4000 cm^{-1}) of solid samples were obtained on a Thermo Nicolet Avatar 360 FT-IR spectrophotometer as KBr pellets. Electronic absorption spectra were recorded from 190 to 820 nm (HP 8452A diode array, UV/vis spectrophotometer). Elemental analyses were performed by RuMega Resonance Labs (San Diego, CA).

Computational Details. All DFT calculations were carried out using the Amsterdam Density Functional program package ADF, release 2002.01.[45−47] The Vosko, Wilk, and Nusair (VWN) local density approximation,[57] the Becke exchange correlation,[58] and the Perdew correlation[59] were used. The calculation also included scalar relativistic effects (ZORA)[60] for all atoms. Uncontracted Slater-type orbitals (STOs)[61] were used as basis functions: Cu, triple-ζ basis set augmented with a set of p functions and frozen core 2p; Ag, triple-ζ basis set augmented with a set of p functions and frozen core 3d; Au, triple-ζ basis set augmented with a set of p functions and frozen core 4d; N, triple-ζ basis set augmented with a set of d functions and frozen core 1s; C, triple ζ-basis set augmented with a set of d functions and frozen core 1s; H, triple-ζ basis set augmented with a set of p functions. This basis combination is denoted as TZP in the ADF program. For the analyses of the metal−ligand bonds, Ziegler and Rauk's energy decomposition scheme was employed.[50,51]

Molecular orbitals were visualized using the MOLDEN program package (http://www.cmbi.kun.nl/~schaft/molden/molden.html).

Synthesis. Starting Materials. *N*-Methylimidazole (Acros), ammonium hexafluorophosphate (Acros), tetrabutylammonium hexafluorophosphate (Acros), potassium *tert*-butoxide (Acros), silver oxide (Fisher), copper(I) bromide (Aldrich), copper(I) trifluoromethanesulfonate (Aldrich), (dimethyl sulfide)gold(I) chloride (Aldrich), and *n*-butyllithium (2.5 M in hexane; Aldrich) were obtained from commercial sources and used as received. Benzylpotassium was prepared according to the methods described in the literature.[62] 1,1,1-Tris(bromomethyl)ethane was synthesized by bromination of the corresponding 1,1,1-tris(hydroxymethyl)ethane (Acros). $[H_3TIME^{Me}](Br)_3$ (**1a**), $[H_3TIME^{Me}](PF_6)_3$ (**1b**), and $[(TIME^{Me})_2Ag_3](PF_6)_3$ (**3**) were synthesized as described previously.[29]

1,1,1-Tris[(*p*-toluenesulfonato)methyl]ethane. 1,1,1-Tris(hydroxymethyl)ethane (168.4 g, 1.4 mol) and pyridine (500 mL) were added to a 3 L three-necked flask. The flask was equipped with a mechanical stirrer, a thermometer, and a 500 mL addition funnel. The solution was then cooled to 0 °C over an ice−water bath. *p*-Toluenesulfonyl chloride (820 g, 4.2 mol) in 500 mL of pyridine was slowly added to the mixture via an addition funnel (the temperature of the solution was kept below 45 °C during the addition). The addition was completed in 1 h, and the mixture was removed from the ice−water bath and stirred for another 1 h. The resulting solution was then added slowly to a mixture of 1 L of HCl and 500 mL of methanol. The white solid that precipitated was collected by filtration and washed with water and methanol (800 g; yield 98%).

1,1,1-Tris(bromomethyl)ethane. 1,1,1-Tris[(*p*-toluenesulfonato)methyl]ethane (519 g, 0.9 mol) and sodium bromide (483 g, 4.7 mol) were added to a 3 L flask, and the mixture was refluxed for 16 h. The resulting suspension was cooled to room temperature, and 500 mL of water was added. The organic phase was extracted with benzene and evaporated to give a white powder (139 g; yield 50%).

$[H_3TIME^{Me}](Br)_3$ (1a). A 50 mL flask was charged with 1,1,1-tris(bromomethyl)ethane (8.5 g, 0.026 mol) and *N*-methylimidazole (10.8 g, 0.131 mol), and the mixture was heated to 150 °C for 1 day, during which time a white solid formed. The solid was filtered off, washed with diethyl ether, and recrystallized from methanol (12.6 g; yield 88%). ^{1}H NMR (400 MHz, d_6-DMSO, 20 °C): δ 9.28 (s, 3H), 7.89 (s, 3H), 7.81 (s, 3H), 4.37 (s, 6H), 3.89 (s, 9H,), 0.99 ppm (s, 3H). ^{13}C NMR (100 MHz, d_6-DMSO, 20 °C): δ 137.5, 123.6, 123.4, 52.9, 38.3, 36.0, 18.9 ppm. Anal. Calcd for $C_{17}H_{27}N_6Br_3 \cdot 1.5H_2O$: C, 35.07; H, 5.19; N, 14.44. Found: C, 35.42; H, 5.51; N, 14.04.

$[H_3TIME^{Me}](PF_6)_3$ (1b). NH_4PF_6 (0.88 g, 5.4 mmol) was added to a solution of **1a** (1 g, 1.8 mmol) in 30 mL of methanol. The white hexaflurophosphate salt precipitated immediately and was collected by filtration, washed with small portions of cold methanol, and dried under vacuum (1.3 g; yield 96%). ^{1}H NMR (400 MHz, d_6-DMSO, 20 °C): δ 9.12 (s, 3H), 7.82 (s, 3H), 7.68 (s, 3H), 4.26 (s, 6H), 3.89 (s, 9H), 0.93 ppm (s, 3H). ^{13}C NMR (100 MHz, d_6-DMSO, 20 °C): δ 137.8, 123.8, 123.5, 52.7, 38.3, 36.0, 17.1 ppm. Anal. Calcd for $C_{17}H_{27}F_{18}N_6P_3$: C, 27.21; H, 3.62; N, 11.20. Found: C, 26.99; H, 3.94; N, 11.23.

$[(TIME^{Me})_2Ag_3](PF_6)_3$ (3). 1b (1.08 g, 1.44 mmol) was dissolved in 100 mL of DMSO, and to this solution was added Ag_2O (0.52 g, 2.24 mmol). The mixture was heated to 75 °C for 12 h. The resulting suspension was filtered through Celite, and to the filtrate was added an equal amount of water to give

(55) Arduengo, A. J.; Gamper, S. F.; Calabrese, J. C.; Davidson, F. *J. Am. Chem. Soc.* **1994**, *116*, 4391−4394.
(56) Arduengo, A. J.; Tamm, M.; Calabrese, J. C. *J. Am. Chem. Soc.* **1994**, *116*, 3625−3626.
(57) Vosko, S. H.; Wilk, L.; Nusair, M. *Can. J. Phys.* **1980**, *58*, 1200−1211.
(58) Becke, A. D. *Phys. Rev. A* **1988**, *38*, 3098−3100.
(59) Perdew, J. P. *Phys. Rev. B* **1986**, *33*, 8822−8824.
(60) Van Lenthe, E.; Ehlers, A.; Baerends, E. J. *J. Chem. Phys.* **1999**, *110*, 8943−8953.
(61) Snijders, J. G.; Vernooijs, P.; Baerends, E. J. *At. Data Nucl. Tables* **1981**, *26*, 483−509.
(62) Schlosser, M.; Hartmann, J. *Angew. Chem.* **1973**, *85*, 544−545.

a white powder. The solid was collected by filtration, washed with diethyl ether, and dried under vacuum (0.67 g, yield 67%). ^{1}H NMR (400 MHz, d_6-DMSO, 20 °C): δ 7.55 (s, 3H), 7.49 (s, 3H), 4.44 (s, br, 3H), 4.20 (s, br, 3H), 3.90 (s, 9H), 1.24 ppm (s, 3H). ^{13}C NMR (100 MHz, d_6-DMSO, 20 °C): δ 182.5, 123.6, 123.2, 59.0, 40.4, 38.2, 18.1 ppm. Anal. Calcd for $C_{34}H_{48}N_{12}Ag_3P_3F_{18}$: C, 29.52; H, 3.50; N, 12.15. Found: C, 29.26; H, 3.46; N, 11.77.

[(TIME^{Me})$_2$Cu$_3$](PF$_6$)$_3$ (4). Method A. A solution of copper(I) bromide (130 mg, 0.9 mmol) in acetonitrile was added dropwise to a solution of **3** (418.2 mg, 0.3 mmol) in 10 mL of acetonitrile. A white precipitate of AgBr formed upon addition of the copper(I) salt. The mixture was filtered through Celite, and to the filtrate was added 50 mL of ether to give a white crystalline powder. The solid was collected by filtration, washed with diethyl ether, and dried under vacuum (210 mg; yield 56%).

Method B. A solution of 3 equiv of base (*n*-butyllithium, potassium *tert*-butoxide, or benzylpotassium) in THF was added dropwise to a suspension of **1b** (365 mg, 0.66 mmol) in 5 mL of THF. A clear colorless solution was formed upon addition of the base. Within 30 min, the solution turned orange-red. The resulting solution was filtered, and copper triflate (129 mg, 0.25 mmol) was added to the filtrate. A light brown precipitate formed immediately. The solid was filtered off and dissolved in 10 mL of acetonitrile, and to the filtered solution was added tetrabutylammonium hexaflurophosphate (1 g, 2.6 mmol). The mixture was stirred for 5 min, and 50 mL of diethyl ether was added to cause precipitation of **4** as an off-white powder. The precipitate was collected by filtration, washed with diethyl ether, and dried under vacuum (110 mg; yield 27%). Colorless crystals suitable for X-ray diffraction analysis were grown by slow diethyl ether diffusion into a saturated solution of **4** in acetonitrile at room temperature. ^{1}H NMR (400 MHz, d_6-DMSO, 20 °C): δ 7.49 (s, 3H), 7.44 (s, 3H), 4.55 (s, br, 3H), 4.16 (s, br, 3H), 3.93 (s, 9H), 1.25 ppm (s, 3H). ^{13}C NMR (100 MHz, d_6-DMSO, 20 °C): δ 178.0, 123.0, 58.6, 40.1, 37.7, 18.1 ppm. Anal. Calcd for $C_{34}H_{48}N_{12}Cu_3P_3F_{18}$: C, 32.66; H, 3.89; N, 13.44. Found: C, 31.59; H, 4.14; N, 12.94.

[(TIME^{Me})$_2$Au$_3$](PF$_6$)$_3$ (5). A solution of Au(SMe$_2$)Cl (122 mg, 0.41 mmol) in acetonitrile was added dropwise to a solution of **3** (190.1 mg, 0.14 mmol) in 10 mL of acetonitrile. A white precipitate of AgBr formed upon addition of the gold(I) salt. The mixture was filtered through Celite, and to the filtrate was added 20 mL of ether to give a white crystalline powder. The solid was collected by filtration, washed with diethyl ether, and dried under vacuum (110 mg; yield 48%). Colorless crystals suitable for X-ray diffraction analysis were grown by slow diethyl ether diffusion into a saturated solution of **5** in acetonitrile at room temperature. ^{1}H NMR (400 MHz, d_6-DMSO, 20 °C): δ 7.61 (s, 3H), 7.48 (s, 3H), 4.80 (d, 3H), 4.20 (d, 3H), 3.94 (s, 9H), 1.26 ppm (s, 3H). ^{13}C NMR (100 MHz, d_6-DMSO, 20 °C): δ 183.8, 123.6, 57.6, 40.2, 37.5, 22.5 ppm. Anal. Calcd for $C_{34}H_{48}N_{12}Au_3P_3F_{18}$: C, 24.74; H, 2.93; N, 10.18. Found: C, 23.45; H, 2.62; N, 9.42.

Crystallographic Details for [(TIME^{Me})$_2$Cu$_3$](PF$_6$)$_3$ (4). A crystal of dimensions 0.28 × 0.26 × 0.17 mm^3 was mounted on a glass fiber. A total of 19 034 reflections ($-24 \le h \le 24$, $-24 \le k \le 23$, $-28 \le l \le 29$) were collected at $T = 100(2)$ K in the θ range of 2.17−27.53°, of which 1773 were unique ($R_{int} = 0.0207$); Mo Kα radiation was used ($\lambda = 0.710\,73$ Å). The structure was solved by direct methods (Shelxtl version 6.10, Bruker AXS, Inc., 2000). All non-hydrogen atoms were refined anisotropically. Hydrogen atoms were placed in calculated idealized positions. The residual peak and hole electron densities were 0.591 and −0.205 e Å^{-3}. The absorption coefficient was 1.595 mm^{-1}. The least-squares refinement converged normally with residuals of $R(F) = 0.0275$, $R_w(F^2) = 0.0788$, and GOF = 1.112 ($I > 2\sigma(I)$). Crystal data: $C_{17}H_{24}Cu_{1.50}F_9N_6P_{1.50}$, space group $R\bar{3}c$, rhombohedral, $a = b = 18.593(2)$ Å, $c = 23.059(4)$ Å, $\alpha = \beta = 90°$, $\gamma = 120°$, $V = 6903.3(18)$ Å^3, $Z = 12$, $\rho_{calcd} = 1.805$ Mg/m^3.

Crystallographic Details for [(TIME^{Me})$_2$Au$_3$](PF$_6$)$_3$ (5). A crystal of dimensions 0.22 × 0.10 × 0.04 mm^3 was mounted on a glass fiber. A total of 14 183 reflections ($-21 \le h \le 21$, $-21 \le k \le 20$, $-26 \le l \le 26$) were collected at $T = 100(2)$ K in the θ range of 2.16−23.99°, of which 1198 were unique ($R_{int} = 0.0567$); Mo Kα radiation was used ($\lambda = 0.710\,73$ Å). The structure was solved by direct methods (Shelxtl Version 6.10, Bruker AXS, Inc., 2000). All non-hydrogen atoms were refined anisotropically. Hydrogen atoms were placed in calculated idealized positions. The residual peak and hole electron densities were 1.967 and −0.621 e Å^{-3}. The absorption coefficient was 9.836 mm^{-1}. The least-squares refinement converged normally with residuals of $R(F) = 0.0416$, $R_w(F^2) = 0.01078$, and GOF = 1.038 ($I > 2\sigma(I)$). Crystal data: $C_{34}H_{48}Au_3F_{18}N_{12}P_3$, space group $R\bar{3}c$, rhombohedral, $a = b = 18.3767(14)$ Å, $c = 23.425(4)$ Å, $\alpha = \beta = 90°$, $\gamma = 120°$, $V = 6850.9(13)$ Å^3, $Z = 6$, $\rho_{calcd} = 2.401$ Mg/m^3.

Acknowledgment. This work was supported by the University of California, San Diego. We are grateful for the support by Dr. Christina Hauser over the years. We also thank Dr. Peter Gantzel for help with the crystallography.

Supporting Information Available: Figures giving UV−vis data of compounds **1b** and **3**−**5** and an ORTEP plot of **5** and complete structural parameters for **4** and **5** as CIF files. This material is available free of charge via the Internet at http://pubs.acs.org.

OM0341855